INORGANIC CHEMISTRY
FRONTIERS

RESEARCH ARTICLE

View Article Online
View Journal | View Issue

Cite this: *Inorg. Chem. Front.*, 2019, **6**, 808

Molecular-salt hybrids; integration of ammonia borane into lithium halides†

Irene Cascallana-Matías,[a,b] Joachim Breternitz,‡[a] Annabelle Baker,[c] Hallam Davis,[a] Edmund J. Cussen§[b] and Duncan H. Gregory *[a]

Received 23rd January 2019,
Accepted 16th February 2019

DOI: 10.1039/c9qi00099b

rsc.li/frontiers-inorganic

New molecular-salt-like hybrids contain ammonia borane (AB) in co-existence with lithium halides in single lattices. [LiI](NH_3BH_3) and [LiI](NH_3BH_3)$_2$ are members of a generic [LiX]$_m$(AB)$_n$ (X = I^-, BH_4^-; *m*, *n* = integer) materials family which release hydrogen on decomposition and demonstrate Li^+-ion conductivity more than two orders of magnitude higher than either $LiBH_4$ or LiI.

Light metal complex hydrides such as lithium alanates and borohydrides have attracted immense interest given the high values of pseudo-reversible gravimetric hydrogen capacity that are possible.[1–4] Moreover, the decomposition and release of hydrogen from a number of complex hydrides such as lithium borohydride is linked to a transition to a fast lithium ion conducting state.[5,6] $LiBH_4$ has an inherently low Li^+ ion conductivity under ambient conditions that can be improved *via* phase transitions that occur at higher temperature (HT) or pressure (HP). The HT polymorph can be stabilised at room temperature by partial replacement of $(BH_4)^-$ with Br^- or I^-, leading to an increase in conductivity by several orders of magnitude at 30 °C.[7,8] Other hydrides of even higher complexity such as amide borohydrides can exhibit Li ion transport into the superionic regime with values of conductivity at ambient and elevated temperatures far exceeding those of the equivalent component binary lithium compounds themselves.[9,10] In fact, from a practical standpoint, complex borohydrides exhibit surprisingly good compatibility with Li (or Na) electrodes and a high electrochemical stability.[5] Moreover, the electrolyte–electrode interface is not difficult to fabricate, simplifying manufacture of battery architectures, although coatings between both components are required.[6]

Similar to the complex hydrides, the molecular hydride, ammonia borane (AB), NH_3BH_3, has long been considered as a promising candidate for high capacity hydrogen storage applications.[11–14] AB has a low molecular weight (30.7 g mol^{-1}), satisfactory air-stability and is thermally stable above 100 °C. Several lithium aminoboranes have been characterised in terms of their hydrogen storage properties,[15] but unlike the borohydrides, their Li-ion conductivity is unknown.

Here, we investigate the Li-ion transport properties of molecular hydride-metal hydride/halide materials for the first time. The design of these solids incorporates molecular and ionic components in hybrid structures and as part of this study we report the Li-ion transport properties of the ammonia borane borohydride, $[LiBH_4]_2NH_3BH_3$ and the related lithium diamidoborane borohydride, $Li(BH_3NH_2BH_2NH_2BH_3)$; two compounds formerly considered as hydrogen storage materials. Moreover, by following a hybrid materials design strategy, we demonstrate that it is possible to synthesise two novel lithium ammonia borane iodides, LiI[NH_3BH_3] and LiI[NH_3BH_3]$_2$. The structure, thermal stability and decomposition behaviour of the compounds was elucidated and their Li-ion transport properties compared to the AB- and diamidoborane borohydrides above. The behaviour of the materials can be rationalised in terms of their composition and hybrid crystal structures.

$[LiBH_4]_2NH_3BH_3$ (**1**) and $Li(BH_3NH_2BH_2NH_2BH_3)$ (**2**) were synthesised following the same procedures reported by Rush *et al.* and Grochala *et al.*, respectively.[16,17] The new lithium AB iodides, LiI(NH_3BH_3) (**3**) and LiI(NH_3BH_3)$_2$ (**4**) were prepared mechanochemically from stoichiometric quantities of LiI and NH_3BH_3. A preliminary assessment of results from a series of LiI–NH_3BH_3 mixtures revealed that different compounds likely formed by varying the molar ratio of the starting materials. Powder X-ray diffraction (PXD; ESI Fig. S14†) revealed that milling of 1 : 1 and 1 : 2 LiI : AB mixtures produced two new crystalline phases, nominally LiI(NH_3BH_3) (**3**) and LiI(NH_3BH_3)$_2$ (**4**). Given the distinctive B–H and N–H stretching (ν) and deformation (δ) modes, Raman spectroscopy is an excellent probe for the study of AB-containing materials. Brief

[a]*WestCHEM, School of Chemistry, University of Glasgow, Glasgow, G12 8QQ, UK. E-mail: Duncan.Gregory@Glasgow.ac.uk*
[b]*WestCHEM, Dept of Pure and Applied Chemistry, University of Strathclyde, Glasgow G1 1XL, UK*
[c]*Diamond Light Source, Harwell Oxford, Didcot, Oxfordshire OX11 0QX, UK*
†Electronic supplementary information (ESI) available. See DOI: 10.1039/c9qi00099b
‡Present address: Structure and Dynamics of Energy Materials, Helmholtz-Zentrum Berlin für Materialien und Energie, Hahn-Meitner-Platz 1, 14109 Berlin, Germany.
§Present address: Dept of Chemical & Biological Engineering, University of Sheffield, Mappin Street, Sheffield S1 3JD, UK.

inspection of the spectra strongly suggests that AB is intact within both **3** and **4** (and that B–N–H species exist in **1** and **2** as expected) (ESI†).

The indexing of laboratory PXD patterns was confirmed from synchrotron PXD data. The latter were used for precise structure refinement (ESI†). The new phases **3** and **4** both crystallise in the monoclinic system; the former in space group $P2_1/c$ (a = 4.39140(1) Å, b = 16.17291(5) Å, c = 7.15685(2) Å, β = 101.52(2)°), the latter in space group $C2$ (a = 12.40709(4) Å, b = 7.22117(3) Å, c = 4.42025(2) Å, β = 106.21(1)°). The iodine position and good estimates for the B and N positions were found after solving each of the structures with the charge flipping algorithm in Superflip.[18] Li positions in **3** and **4** were subsequently tentatively located from difference Fourier maps. The structures of **1–4** are shown in Fig. 1.

Combined thermogravimetric-differential thermal analysis (TG-DTA) experiments were performed on both new materials **3** and **4** to determine their thermal stability and decomposition behaviour prior to performing AC impedance measurements (Table 1 and ESI†). Both **3** and **4** exhibit sharp endotherms above 100 °C with no concurrent mass loss (with maxima at 119.5 °C and 114.2 °C, respectively) and the two compounds each demonstrate two exothermic decomposition steps thereafter between *ca.* 120–200 °C (with mass losses of *ca.* 13 and 16.5 wt%, respectively). The PXD patterns collected for **3** and **4** after the two decomposition steps show the formation of LiI as the only crystalline product (ESI Fig. S19 and S20†), suggesting that both exothermic events originate from the decomposition of AB. This evidence would also imply that the lower temperature endothermic event in the profiles of **3** and **4** likely arises from the decomposition of the compounds into their respective ionic (LiI) and molecular (AB) components (coupled with melting of AB). The thermal stability of **1** and **2** were measured for comparison (Table 1 and ESI†). Both materials also exhibit mass losses between 120–200 °C as has been documented previously.[16,17] We note that in both **1** and **2** these decomposition steps are exothermic as seen in **3** and **4** and that in each case the exothermic process is preceded by an endothermic one (at *ca.* 111 °C and 136 °C for **1** and **2**, respectively). We again associate the endotherms with decomposition (for **1**) and/or melting. Hydrogen was the predominant gaseous decomposition product but borazine, diborane and ammonia were also evolved.

All conductivity measurements were performed from room temperature to the point of the first endothermic events (the respective melting/decomposition points). Activation energies were extracted from Arrhenius plots for **1** and **2** between 343–403 K and **3** and **4** between 293–343 K, respectively. Above these upper temperature limits further evidence of decomposition was observed in the conductivity data. For **1**, for example, where thermal analysis suggested two endotherms prior to mass loss (ESI Fig. S4†), a steep drop in conductivity is observed at *ca.* 95–100 °C. This is commensurate with decomposition of **1** into AB and LT-$LiBH_4$ (the "low temperature" polymorph) and the subsequent transition of the LT-phase to HT-$LiBH_4$ before AB begins thermal decomposition. The conductivity data for **1–4** are shown in Fig. 2 and Table 2.

Impedance data analysed in the complex plane showed a semicircle at high frequencies and a linear response at low frequencies characteristic of ionic conductivity and ion blocking electrodes. At lower temperatures two semicircles were

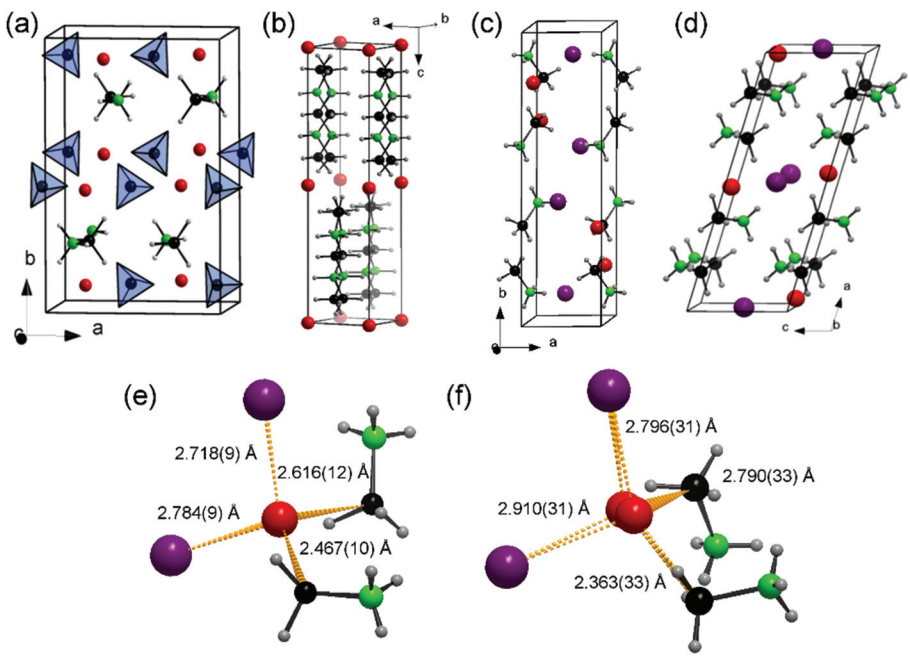

Fig. 1 Crystal structures of: (a) $[LiBH_4]_2[NH_3BH_3]$ (**1**); (b) $Li(BH_3NH_2BH_2NH_2BH_3)$ (**2**); (c) $[LiI][NH_3BH_3]$ (**3**) and (d) $[LiI][NH_3BH_3]_2$ (**4**). Detail of the distorted tetrahedral coordination environment of Li^+ in (e) $[LiI][NH_3BH_3]$ (**3**) and (f) $[LiI][NH_3BH_3]_2$ (**4**). Li, I, N, B and H are represented as red, purple, green, black and grey spheres, respectively.

Table 1 Thermal decomposition characteristics of **1–4** from *ca.* 25–200 °C

	Material					
	1	$[LiBH_4]_2NH_3BH_3$ [16]	**2**	$Li[BH_3NH_2BH_2NH_2BH_3]$ [17]	**3**	**4**
Formula mass/g mol^{-1}	74.46	74.46	81.38	81.38	164.81	195.46
1st endotherm peak T/°C	97.8	[a]	136.1	—	119.5	114.2
Mass loss onset T/°C	111.2	105	136.1	140	132.3	123.5
Mass loss/wt%	27.4	27	34.0	9	11.9	16.4
Gases evolved	H_2, NH_3, $B_3H_6N_3$, B_2H_6	H_2, NH_3, $B_3H_6N_3$, B_2H_6	H_2, $B_3H_6N_3$, B_2H_6, NH_3	H_2	H_2, $B_3H_6N_3$, NH_3, B_2H_6	H_2, $B_3H_6N_3$, NH_3, B_2H_6
Decomposition products (XRD)	$LiBH_4$	$LiBH_4$	[b]	$LiBH_4$	LiI	LiI
Decomposition products (Raman)	$(NHBH)_n$ $LiBH_4$	[a]	$(NH_2BH_2)_n$ $(NHBH)_n$ $LiBH_4$	[a]	$(NH_2BH_2)_n$ $(NHBH)_n$	$(NHBH)_n$

[a] Not reported. [b] Amorphous.

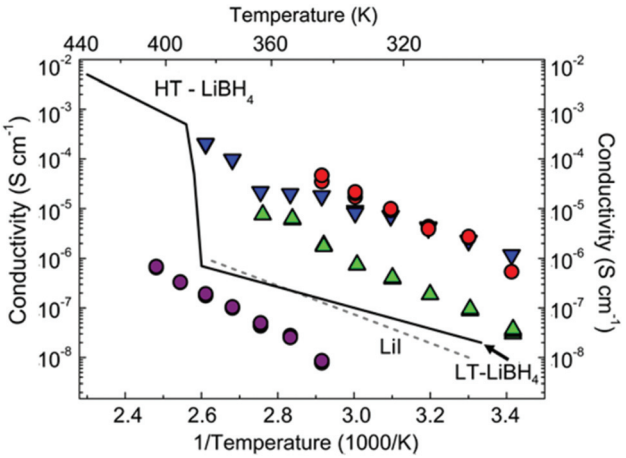

Fig. 2 Arrhenius plots of total conductivity against reciprocal temperature (and temperature) for **1–4**. The plotted conductivity represents the sum of the grain boundary and bulk contributions. The temperature dependence of the conductivity for LiI[7] and $LiBH_4$ [19] is shown for comparison. **1–4** are represented in red, magenta, green and blue respectively.

Table 2 Ionic conductivity at 343 K (σ_{343}) and Li^+ ion transport activation energies (E_a) for **1–4**

Material	σ_{343}/S cm^{-1}	E_a/eV
$[LiBH_4]_2[NH_3BH_3]$ (**1**)	2.83×10^{-5}	0.71(3)
$Li[BH_3NH_2BH_2NH_2BH_3]$ (**2**)	4.11×10^{-9}	0.86(1)
$[LiI][NH_3BH_3]$ (**3**)	1.80×10^{-6}	0.69(1)
$[LiI][NH_3BH_3]_2$ (**4**)	1.79×10^{-5}	0.48(1)

observed, suggesting intra- and inter-grain transport could be resolved. However, the high frequency semicircle moved beyond the measurement range at higher temperatures and so the data were analysed using an equivalent electrical circuit to extract the values for the total resistivity. **2** has conductivity several orders of magnitude lower than that of the other materials, with a correspondingly higher activation energy for Li^+ ion conduction.

The remaining compounds, containing molecular NH_3BH_3 and either I^- or $[BH_4]^-$ as spherical anions, exhibit superior conductivities with the best performance demonstrated by **1** and **4**. In fact, the activation energy for **4** is slightly lower than the values reported for the fast ion conductors HT-$LiBH_4$ (0.53 eV)[20] and $Li_3(NH_2)_2I$ (0.58 eV).[10] The ionic conductivity for **4** increases by *ca.* 2 orders of magnitude between 343–383 K and the absolute value is only slightly lower than that observed for iodide-stabilised $LiBH_4$ at these temperatures.

It is well-known that open structures with available interstitial positions are often favourable for ionic conductivity.[21] It is perhaps not surprising, therefore that **2** has the lowest Li^+ ion conductivity of the materials studied given the relatively bulky anions and the restricted space available for lithium to diffuse. The closest Li–Li distance in **2** is 4.02(1) Å and the average separation between $[BH_3NH_2BH_2NH_2BH_3]^-$ species within anionic layers in the crystal structure of **2** is ~4.0 Å which is likely to be insufficient to allow the Li^+ ions to pass smoothly.[17,22] The "pseudo-layered" materials, **1** and **4**, exhibit the best ionic conductivity at all temperatures. It is interesting to note that the "ionic section" of the structure of **1** closely resembles the anion and cation arrangement in the fast ion conducting hexagonal HT phase of $LiBH_4$ rather than that in orthorhombic LT-$LiBH_4$, where the conductivity is 10^3–10^4 times lower. Hence, integrating AB into the $LiBH_4$ lattice (or alternatively "implanting" $LiBH_4$ within the AB lattice) effectively drives the LT-HT phase transition at reduced temperature much as halide substitution does in $LiBH_4$ itself. One might assume therefore that the Li^+ conduction mechanism is also similar and would rely on the cooperative rotational motion of the $[BH_4]^-$ anions. In compound **1**, the BH_4^- complex anions and NH_3BH_3 molecules both act effectively as bridging ligands to connect the Li^+ ions in three dimensions.[23] The closest Li–Li distances are 3.42 Å and 4.05 Å within the $LiBH_4$-type ionic pseudo-layers and 4.30 Å across AB layers. It seems reasonable to envisage anisotropic Li^+ ion conductivity in **1** with faster transport within the ionic pseudo-layers (*ac* plane) than between them (*b*-direction).

Of the iodides, although **4** contains proportionately less lithium, it has a higher total ionic conductivity across the

entire measured temperature range. The segregation of the ionic and molecular sections of the structure in the AB-rich compound **4** are more pronounced than in **3** and similarly to **1**, it contains ionic and molecular pseudo-layers. By contrast to **1** however, the molecular layers in **4** are thicker – 2 AB molecules across (along the long *a*-axis) – and so the structure of **4** is more "AB-like" than **1**, with the segregation of the ionic and molecular parts of the structure seemingly facilitating the migration of the Li^+ ions in the *bc* plane in **4**. There is no such segregation in **3** and the pathways for Li^+ ion conduction would appear to be more restricted and probably limited to one dimension only. Moreover, the structure solution of **4** suggests disorder and hence Li^+ vacancies in the lithium sublattice, providing a further possible rationale for the enhanced ionic conductivity. Given the relatively weak X-ray scattering of Li^+ (in the presence of I^-) and the similarity in scattering power of N and B, it is not possible to draw more definitive conclusions regarding the existence of Li^+ vacancies or whether the AB molecules in **3** and **4** exhibit dynamic (or positional) disorder. From current evidence, it appears that the AB does not play an active part in a cooperative Li^+ ion conductivity mechanism. We intend to clarify this once powder neutron diffraction experiments have been completed. However, the fact that the U_{iso} values of the B and N atoms become physically unreasonable when the atomic positions are exchanged indicates that the AB molecules may be relatively static. An interesting comparison can nonetheless be made to lithium amide halides such as $Li_3(NH_2)_2I$ ($\sigma \approx 1.7 \times 10^{-5}$ S cm^{-1} at room temperature). The Li^+ ion conductivity in $Li_3(NH_2)_2I$ was proposed to be associated with short Li–Li distances and abundant interstitial sites, rather than being influenced by NH_2^- reorientation (for which there was no direct evidence).[10,24] Compound **1** contains a relatively short Li–Li distance (3.42 Å); within the range of distances observed in $Li_3(NH_2)_2I$.[10,24] However, conversely, compound **4** with comparable conductivity to **1**, has no such short Li–Li spacings (with a closest Li–Li distance of *ca.* 4.3 Å), suggesting that the conductivity mechanisms in the AB borohydride and the AB iodides could indeed be different.

In this context, it is also useful to compare the conductivity of **3** and **4** with LiI itself. Rock salt-structured LiI shows only modest ionic conductivity at room temperature.[25] This is despite the fact that the anion has the highest polarizability among the halides.[26] The observed ionic conductivity of LiI is predominantly extrinsic below 180 °C,[25] whereas above 180 °C, its intrinsic conducting behaviour is mediated by Schottky defects. This can be dramatically enhanced in the monohydrate ($LiI{\cdot}H_2O$; with an anti-perovskite structure), where 2/3 of the octahedral Li^+ sites are vacant (or equally the conductivity can be improved by aliovalent doping of Ca^{2+} in LiI).[27] By loose analogy to the hydrate, inserting LiI into a lattice of AB should enlarge the space for Li migration (providing new and available interstitial sites) and enhance ionic conductivity. This would especially appear to be the case in **4** where the activation energy for Li^+ transport is notably lower than in any of the other materials.

Experimental

Full details are provided in the ESI.† $[LiBH_4]_2NH_3BH_3$ (**1**) and $Li(BH_3NH_2BH_2NH_2BH_3)$ (**2**) were synthesised following previously reported procedures.[16,17] The LiI–NH_3BH_3 materials (**3** and **4**) were prepared by ball milling stoichiometric ratios of LiI and NH_3BH_3 in hardened steel jars (50 ml) with 10 hardened steel balls of 10 mm diameter using a Retsch PM100 ball mill. The mixture was milled for 2 h at 250 rpm (400 : 1, ball-to-powder-ratio by mass) to yield white powders.

Powder X-ray diffraction (PXD) data were obtained at room temperature with a Bruker D8 Advance (θ–2θ) diffractometer, using Cu Kα_1 radiation and a step size of 0.017° 2θ over 5–95° 2θ for *ca.* 12 h. Jana2006 was used for the initial Le Bail fitting and space group assignments of the new compounds **3** and **4**.[28] The structures of **3** and **4** were then solved using Superflip within Jana. For **4**, Li positions were tentatively identified from difference Fourier maps. High Resolution synchrotron PXD experiments were performed using beamline I11 (λ = 0.826281(10) Å) and the structures refined against the synchrotron data using the Rietveld method (with GSAS/EXPGUI software).[29,30]

Raman spectra were measured at room temperature using a Horiba Jobin Yvon Raman microscope with a green laser (λ = 532 nm) and employing a hole aperture of 50 μm, 100 g mm^{-1} grating and a synapse CCD detector. Sample morphology and composition were studied using scanning electron microscopy (SEM) (XL 30 ESEM, Philips, 25 kV accelerating voltage with an Oxford Instruments X-act spectrometer for EDX analysis). Thermogravimetric-differential thermal analysis-evolved gas mass spectrometry (TG-DTA-MS; NETZSCH STA 409PC and HIDEN HPR20 mass spectrometer) was performed from room temperature to 473 K at 5 K min^{-1} under an Ar flow. MS signals were monitored with time and temperature.

Electrochemical impedance measurements (Solartron 1260 impedance analyser) were performed on cylindrical pellets on heating, allowing the temperature to equilibrate for ≥1 h before collecting data. Data were analysed using equivalent circuit analysis as implemented in the ZView2 software package.

Conclusions

In summary, ammonia borane halides have been synthesised for the first time and the 2 new iodides can be classified with $[LiBH_4]_2NH_3BH_3$ into a broader family of hybrid compounds, $[LiX]_m(AB)_n$ (X = I^-, BH_4^-; m, n = integer). The materials are stable above 100 °C and decompose to the binary halides (borohydride) with the evolution of hydrogen as the main gaseous product. The Li-ion conductivity of these hybrid hydrides has been determined and exceeds that of the binary respective ionic components by orders of magnitude. The conduction pathways can be tailored through the partition of ionic and molecular sections in these hybrid materials. In principle, Li-ion transport in this class of materials could be further optimised by substitutions in the ionic sub-structure.

Moreover, the control of static and dynamic disorder in the cationic, anionic and molecular sub-lattices should prove pivotal in the design of new Li^+ ion conductors and ultimately potential electrolytes. Indeed, a vast range of new hybrid materials should be accessible with transport properties and stabilities that can be manipulated by the judicious selection of all the component species; cationic, anionic and molecular.

Conflicts of interest

There are no conflicts to declare.

Acknowledgements

The authors thank the Universities of Glasgow and Strathclyde for supporting this work and Mr Nicolás Flores González for assistance with MS data. The synchrotron radiation experiments were performed at the I11 instrument at the Diamond Light Source, Oxfordshire (beamtime award EE13155).

Notes and references

1 S. Orimo, Y. Nakamori, J. R. Eliseo, A. Züttel and C. M. Jensen, *Chem. Rev.*, 2007, **107**, 4111.
2 T. K. Mandal and D. H. Gregory, *Annu. Rep. Prog. Chem., Sect. A: Inorg. Chem.*, 2009, **105**, 21.
3 T. K. Mandal and D. H. Gregory, *Proc. IMechE, Part C: J. Mech. Eng. Sci.*, 2010, **224**(C3), 539.
4 H. Reardon, J. Hanlon, R. W. Hughes, A. Godula-Jopek, T. K. Mandal and D. H. Gregory, *Energy Environ. Sci.*, 2012, **5**, 5951.
5 M. Matsuo and S. Orimo, *Adv. Energy Mater.*, 2011, **1**, 161–172.
6 P. E. Jongh, D. Blanchard, M. Matsuo, T. J. Udovic and S. Orimo, *Appl. Phys. A: Mater. Sci. Process.*, 2016, **122**, 1.
7 H. Maekawa, M. Matsuo, H. Takamura, M. Ando, Y. Noda, T. Karahashi and S. Orimo, *J. Am. Chem. Soc.*, 2009, **131**, 894.
8 I. Cascallana-Matías, D. A. Keen, E. J. Cussen and D. H. Gregory, *Chem. Mater.*, 2015, **27**, 7780.
9 M. Matsuo, A. Remhof, P. Martelli, R. Caputo, M. Ernst, Y. Miura, T. Sato, H. Oguchi, H. Maekawa, H. Takamura, A. Borgschulte, A. Züttel and S. Orimo, *J. Am. Chem. Soc.*, 2009, **131**, 16389.
10 M. Matsuo, T. Sato, Y. Miura, H. Oguchi, Y. Zhou, H. Maekawa, H. Takamura and S. Orimo, *Chem. Mater.*, 2010, **22**, 2702.
11 C. Liu, F. Li, L. P. Ma and H. M. Cheng, *Adv. Mater.*, 2010, **22**, E28.
12 F. H. Stephens, V. Pons and R. T. Baker, *Dalton Trans.*, 2007, **25**, 2613.
13 C. W. Hamilton, R. T. Baker, A. Staubitz and I. Manners, *Chem. Soc. Rev.*, 2009, **38**, 279.
14 A. Staubitz, A. P. Robertson and I. Manners, *Chem. Rev.*, 2010, **110**, 4079.
15 Z. Xiong, C. K. Yong, G. Wu, P. Chen, W. Shaw, A. Karkamkar, T. Autrey, M. O. Jones, S. R. Johnson and P. P. Edwards, *Nat. Mater.*, 2008, **7**, 138.
16 H. Wu, W. Zhou, F. E. Pinkerton, M. S. Meyer, G. Srinivas, T. Yildirim, T. J. Udovic and J. J. Rush, *J. Mater. Chem.*, 2010, **20**, 6550.
17 K. J. Fijalkowski, T. Jaron, P. J. Leszczynski, E. Magos-Palasyuk, T. Palasyuk, M. K. Cyranski and W. Grochala, *Phys. Chem. Chem. Phys.*, 2014, **16**, 23340.
18 L. Palatinus and G. Chapuis, *J. Appl. Crystallogr.*, 2007, **40**, 786.
19 D. Sveinbjornsson, J. S. G. Myrdal, D. Blanchard, J. J. Bentzen, T. Hirata, M. B. Mogensen, P. Norby, S. I. Orimo and T. Vegge, *J. Phys. Chem. C*, 2013, **117**, 3249.
20 W. Li, G. T. Wu, Z. T. Xiong, Y. P. Feng and P. Chen, *Phys. Chem. Chem. Phys.*, 2012, **14**, 1596.
21 C. Sun, J. Liu, Y. Gong, D. P. Wilkinson and J. Zhang, *Nano Energy*, 2017, **33**, 363.
22 R. Owarzany, K. J. Fijalkowski, T. Jaroń, P. J. Leszczyński, Ł. Dobrzycki, M. K. Cyrański and W. Grochala, *Inorg. Chem.*, 2015, **55**, 37.
23 M. Paskevicius, L. H. Jepsen, P. Schouwink, R. Černý, D. B. Ravnsbæk, Y. Filinchuk, M. Dornheim, F. Besenbacher and T. R. Jensen, *Chem. Soc. Rev.*, 2017, **46**, 1565.
24 A. V. Skripov, R. V. Skoryunov, A. V. Soloninin, O. A. Babanova, M. Matsuo and S. Orimo, *J. Phys. Chem. C*, 2015, **119**, 13459.
25 F. W. Poulsen, *Solid State Ionics*, 1981, **2**, 53.
26 A. R. West, *Basic Solid State Chemistry*, John Wiley & Sons Ltd, Chichester, 1988.
27 G. Eichinger, *Solid State Batteries, chapter: conductivity of modified lithium iodide samples*, Springer Netherlands, Dordrecht, 1985.
28 V. Petricek, M. Dusek and L. Palatinus, *Z. Kristallogr.*, 2014, **229**, 345.
29 A. C. Larson and R. B. Von Dreele, General Structure Analysis System (GSAS), Los Alamos National Laboratory Report LAUR, 1994, 86.
30 B. H. Toby, *J. Appl. Crystallogr.*, 2001, **34**, 210.

